Supplemental Figures and Legends

Fig. S1. Structural features and mapping of the autocleavage site of the TgCPL.

A. TgCPL domains are schematically illustrated including a putative N-terminal cytosolic (NTC) domain, signal anchor (SA), propeptide, and catalytic domain. A hydrophilicity plot is shown to indicate the position of the signal anchor, an unusual feature for the papain family members. A putative tyrosine-based endosomal sorting motif (YVSF) and a putative acidic patch (EDD) for ER exit are underlined in the first twenty amino acids of the NTC. Also shown are conserved structural features viewed as a multiple sequence alignment of residues 113-209 (TgCPL numbering) encompassing much of the propeptide, and the well conserved regions immediately surrounding the catalytic triad (C229, H365, and N387; asterisk). Identical residues are shown in black boxes. Highly conserved aromatic residues, the ERFNIN and NFD signatures in the propeptide are indicated by the # symbol. Alignment was performed using ClustalW. The autoactivation cleavage sites are indicated as: TgCPL, black arrows; Papain, white arrowhead; and Cruzipain, black arrowhead.

B. Specificity of anti-TgCPL antibodies. Immunoblot of recombinant enzyme (r100proTgCPL and rTgCPL) and native enzyme (*T. gondii* lysate) probed with RaTgCPLpep. Also shown are blots probed with RαTgCPL and MαTgCPL recognizing the 30 kDa mature form of TgCPL, in addition to the 50 kDa zymogen form (proTgCPL) in parasites extracted with 1% Triton X-100 (Tx-100). Asterisks indicate minor putative non-specific bands. (**C**) Immunoblot of *T. gondii* lysate probed with RαTgCPBpep showing that TgCPB migrates at a different position, therefore suggesting that TgCPL and TgCPB are antigenically distinct. RαTgCPBpep recognizes a peptide epitope in the catalytic domain of TgCPB. All blots are from 12.5% SDS-PAGE gels.

Molecular weight markers are expressed in kDa.

Fig. S2. TgCPL, TgM2AP, and TgMIC3 expression in bradyzoites. Host cell monolayers were infected with ME49 (**A**) or Pru (**B** and **C**) tachyzoites and grown under bradyzoite differentiation conditions. Parasites were fixed and labeled with TRITC-conjugated *Dolichos biflorus* lectin, which stains the bradyzoite cyst wall, or each of the following antibodies: **A**. MαTgCPL, **B.** RαTgM2AP, **C.** MAb T4.2F3 anti-MIC3.

Fig. S3. Similarity of TgRab7 with other Rab7 family members.

A. Molecular phylogenic relationships of TgRab7 with other Rab7 family members from *Plasmodium falciparum* (PfRab7, GenBank CAX64193), *Cryptosporidium parvum* (CpRab7, XP_001388379), *Perkinsus marinus* (PmRab7, EER20423), *Paramecium tetraurelia* (PtRab7, XP_00145889), *Aspergillus oryzae* (AoRab7, XP_001824054), *Saccharomyces cerevisiae* (ScRab7, BAA10973), and *Homo sapiens* (HsRab7 NP_004628). Phylogenetic analysis was carried out using POWER (http://power.nhri.org.tw/power/home.htm; neighbor-joining distance method) and viewed with TREEVIEW (http://darwin.zoology.gla.ac.uk/~rpage/treeviewx/index.html). Branch lengths are drawn to scale (number of amino acid substitutions per site).

B. Multiple sequence alignment of TgRab7 with other Rab7 family members. TgRab7 contains the hallmark conserved features (underlined) of a small GTPase including the effector binding region (R2), GTP-binding regions (R1, R3, R4, and R5), and the C-terminal prenylation element

(CxC or CC). Alignment was created using MUSCLE (http://www.ebi.ac.uk/Tools/muscle/index.html).

Fig. S4. Association of the VAC and late endosomes is dynamic during intracellular replication. Dual staining of TgCPL and TgVP1 during daughter cell formation was studied in fixed RH parasites by double immunolocalization using MαTgCPL and RαTgVP1.

A. The VAC and LE are typically located in the apical region and are often juxtaposed.

B. Elongation of the LE is observed during S phase.

C. Fission of the LE occurs before the initiation of the daughter formation. At this stage the VAC fragmentation is initiated and some small structures are associated with the LE.

D. The newly divided LE is partitioned into the developing daughter parasites, and the fragmented VAC and LE are largely distinct but partial overlap in some parasites.

F. During the final stages of daughter formation, TgCPL is associated with a single VAC that is often adjacent to the LE. Arrows indicate areas of colocalization. Scale bar, 2 μm.

Fig. S5. Organization of the LE and centrosomes during the cell cycle of *Toxoplasma gondii*. Representative immunofluorescence images showing TgVP1 localization in parasites stably expressing GFP-TgCentrin2 during intracellular replication.

A. At the beginning of the cell cycle, the centrosome (indicated by an asterisk) is closely associated with one end of the LE located at the apical end of the parasite.

B. During interphase, the centrosome migrates toward the basal end of the nucleus

C. The centrosome divides at the beginning of S-phase and the LE elongates.

D. The centrosomes move back to the anterior end of the nucleus and re-associate with the LE.

E-F. Fission of the LE occurs before the initiation of the daughter formation. During nuclear division and partition of the newly divided LE, the two centrosomes are found at the inner ends of the compartments.

G. During the final stages of daughter formation, TgVP1 is associated with a single LE associated with the centrosome. Scale bar, 2 μm.

Fig. S6. Low pH supports correct propeptide cleavage of rproTgCPL.

A. Coomassie-stained SDS-PAGE gel showing pH dependent autoactivation of r100proTgCPL to rTgCPL through an apparent intermediate (asterisk). Approximately 1 μg of r100proTgCPL was activated by incubation for 2 h in the presence of 5 mM DTT.

Fig. S7. Morphological changes in the VAC and the late endosome are induced by treatment with pH antagonist drugs. Representative immunofluorescence images showing TgCPL (**A**) or TgVP1 (**B**) localization in RH parasites expressing TgGRASP-mRFP after treatment with pH antagonists. Extracellular parasites were treated with DMSO, 500 nM bafilomycin A1, or 150 mM chloroquine for 15 min at RT, and then incubated for another 1 h at 37°C. The samples were processed for IFA analysis using RαTgCPL or RαTgVP1. Both drugs

caused the enlargement of the VAC and the late endosome. Moreover, chloroquine at the highest concentration tested (150 mM) induced disassemble of the late endosome compartment. Note that both drugs do not alter the structure of the Golgi complex. Arrowheads indicate the apical end of parasite.

Fig. S8. Serine protease inhibitors do not inhibit the proTgM2AP maturation although they significantly decreased and delayed the proTgMIC3 processing. Filter-purified RHΔ*sub1* parasites were pretreated with a solvent control (DMSO), 1mM PMSF, or 10 mM subtilisin inhibitor III for 15 min prior to metabolically labeling for 10 min followed by chase with medium containing cold Met/Cys and the inhibitors for the indicated times. MIC proteins were immunoprecipitated and analyzed by SDS-PAGE.

A. Representative autoradiographs are shown. Arrows indicate the positions of the immature (upper) and mature (lower) forms of each MIC protein.

B-F. Quantification of MIC mat5ration after DMSO (white circles) and 1 mM PMSF (black circles) treatment are shown. Values were calculated as described in Figure legend 6.

Fig. S1

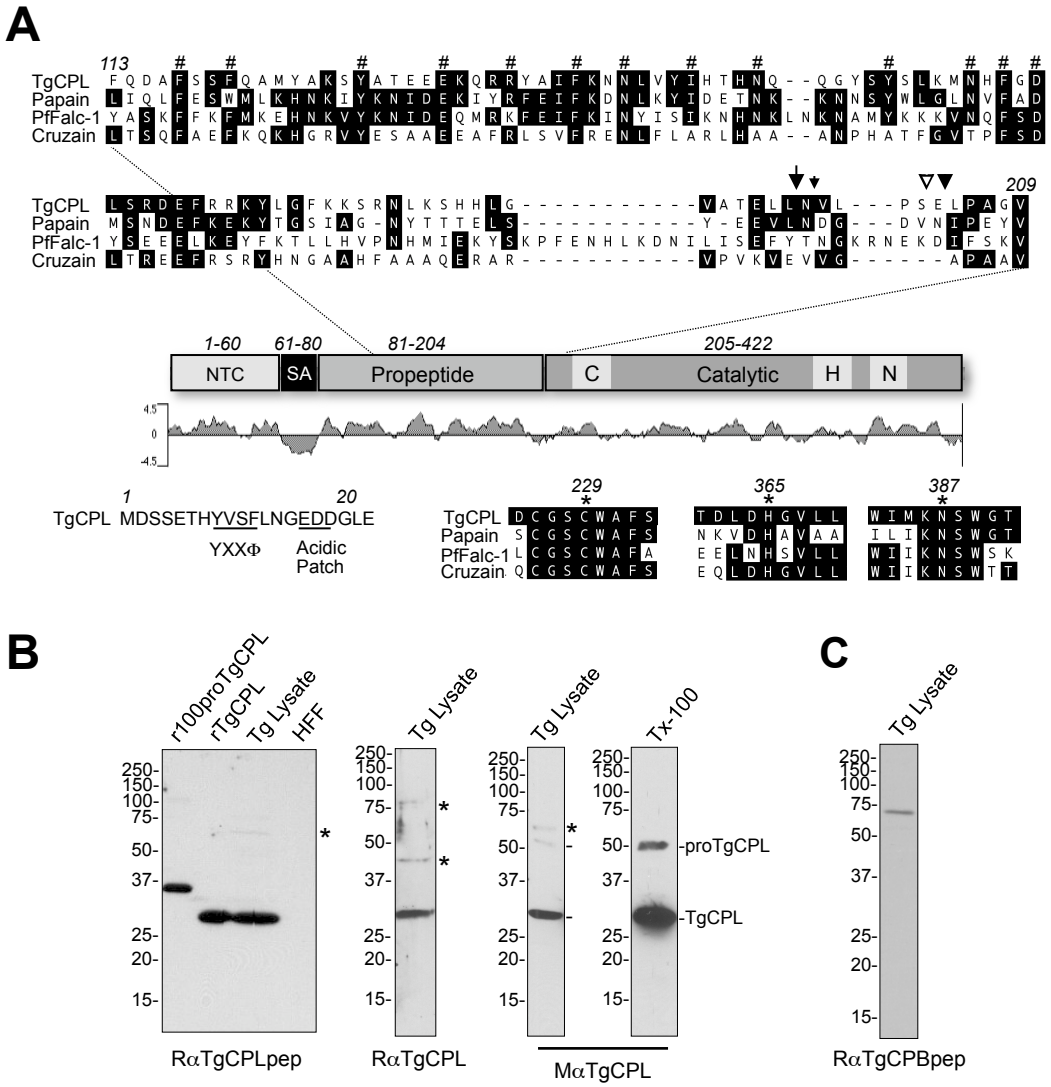
A
TgCPL
Papain
PfFalc-1
Cruzain
1-60
61-80
81-204
205-422
NTC
SA
Propeptide
C
Catalytic
H
N
YXXΦ
Acidic Patch
B
r100proTgCPL
rTgCPL
Tg Lysate
HFF
Tx-100
proTgCPL
TgCPL
RαTgCPLpep
RαTgCPL
MαTgCPL
C
RαTgCPBpep

Fig. S2

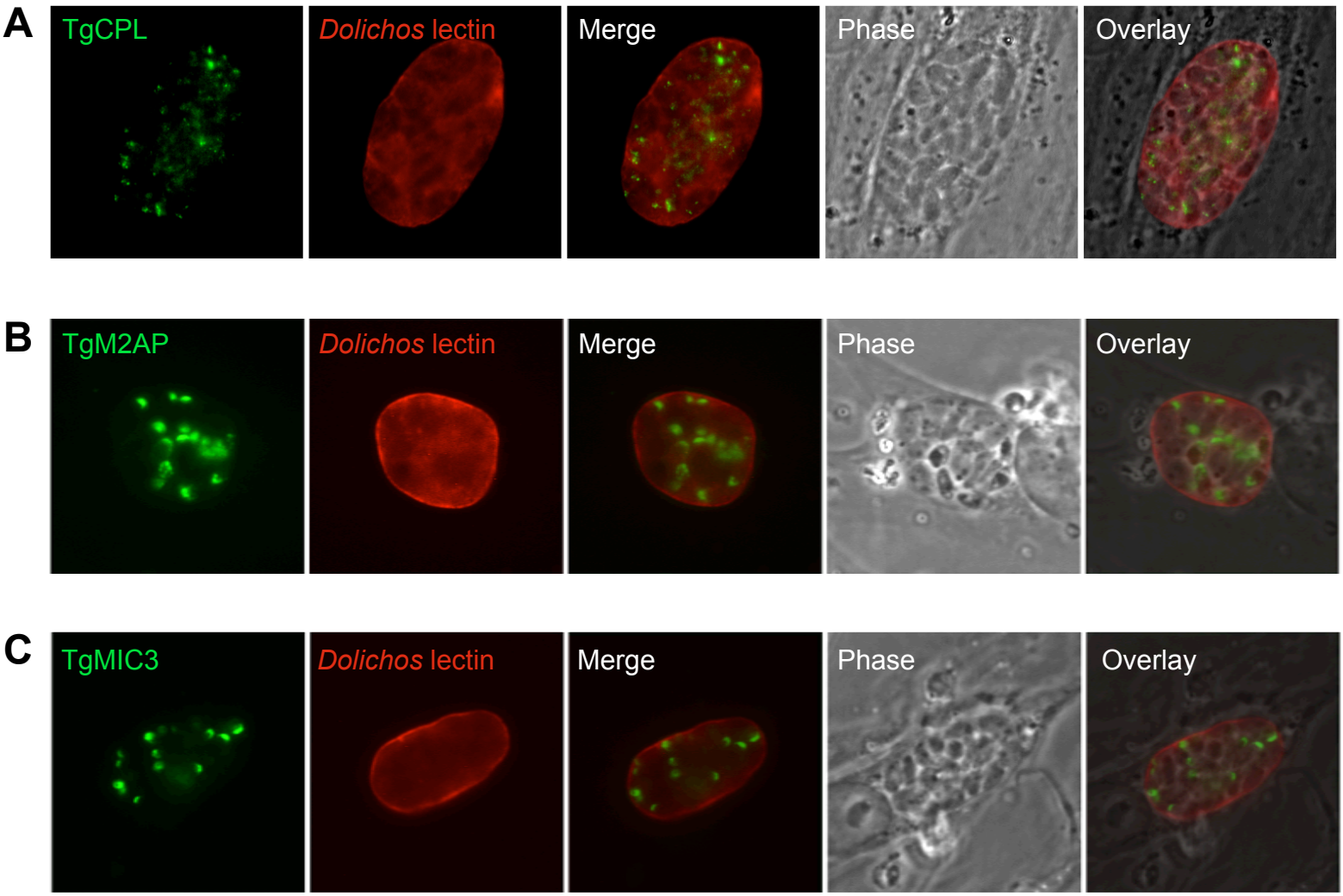
A
TgCPL
Dolichos lectin
Merge
Phase
Overlay
B
TgM2AP
Dolichos lectin
Merge
Phase
Overlay
C
TgMIC3
Dolichos lectin
Merge
Phase
Overlay

Fig. S3

A

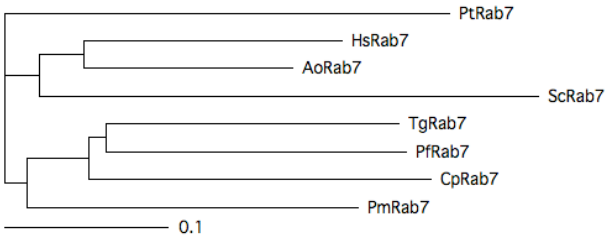
PtRab7
HsRab7
AoRab7
ScRab7
TgRab7
PfRab7
CpRab7
PmRab7
0.1

B

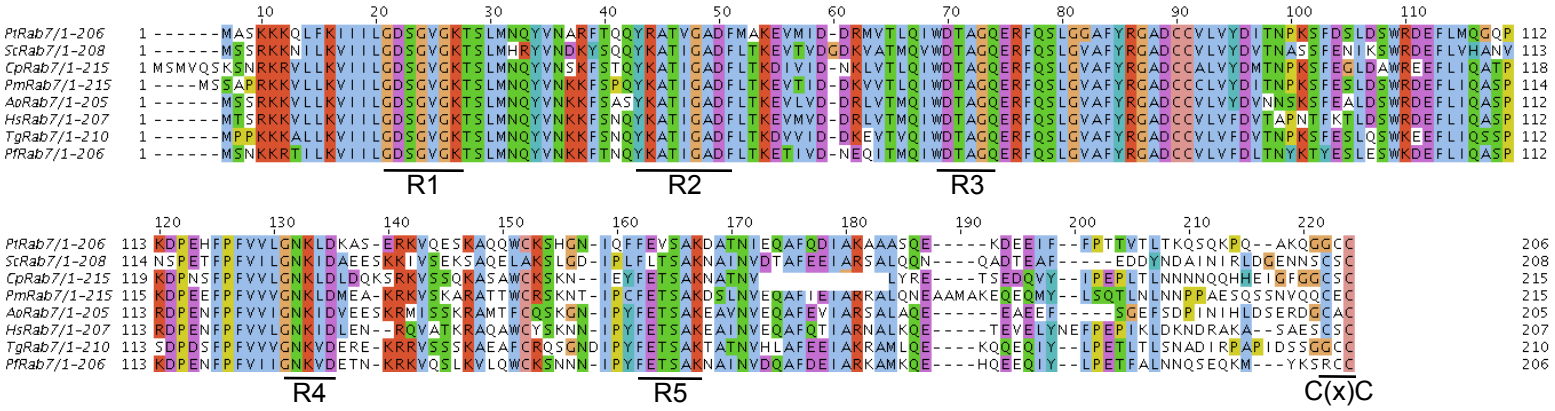
PtRab7/1-206
ScRab7/1-208
CpRab7/1-215
PmRab7/1-215
AoRab7/1-205
HsRab7/1-207
TgRab7/1-210
PfRab7/1-206
R1
R2
R3
R4
R5
C(x)C

Fig. S4

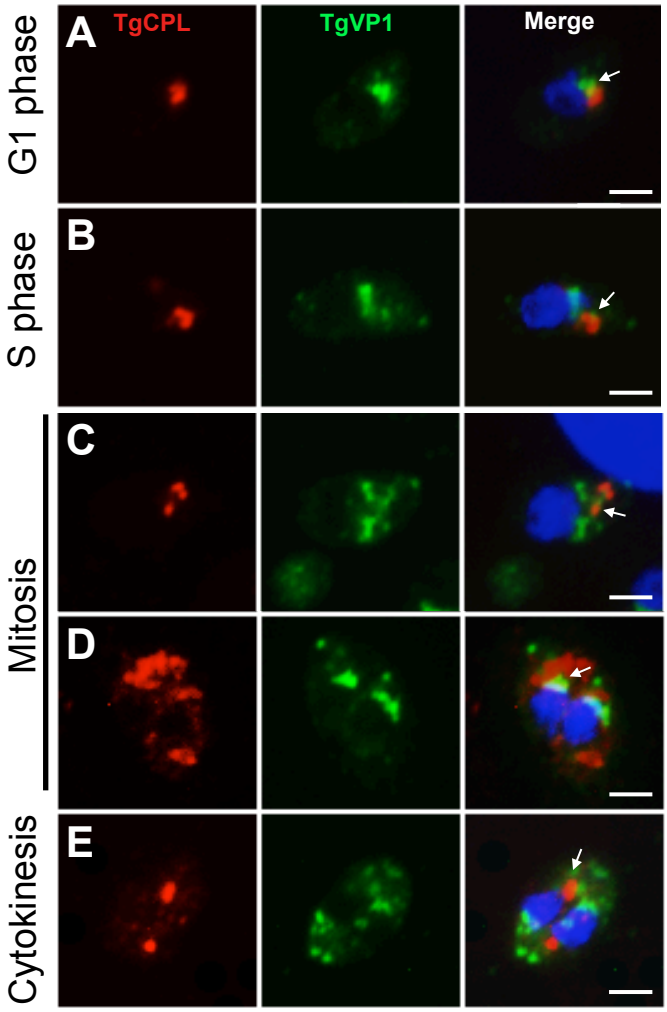
A
TgCPL
TgVP1
Merge
G1 phase
B
S phase
C
D
Mitosis
E
Cytokinesis

Fig. S5

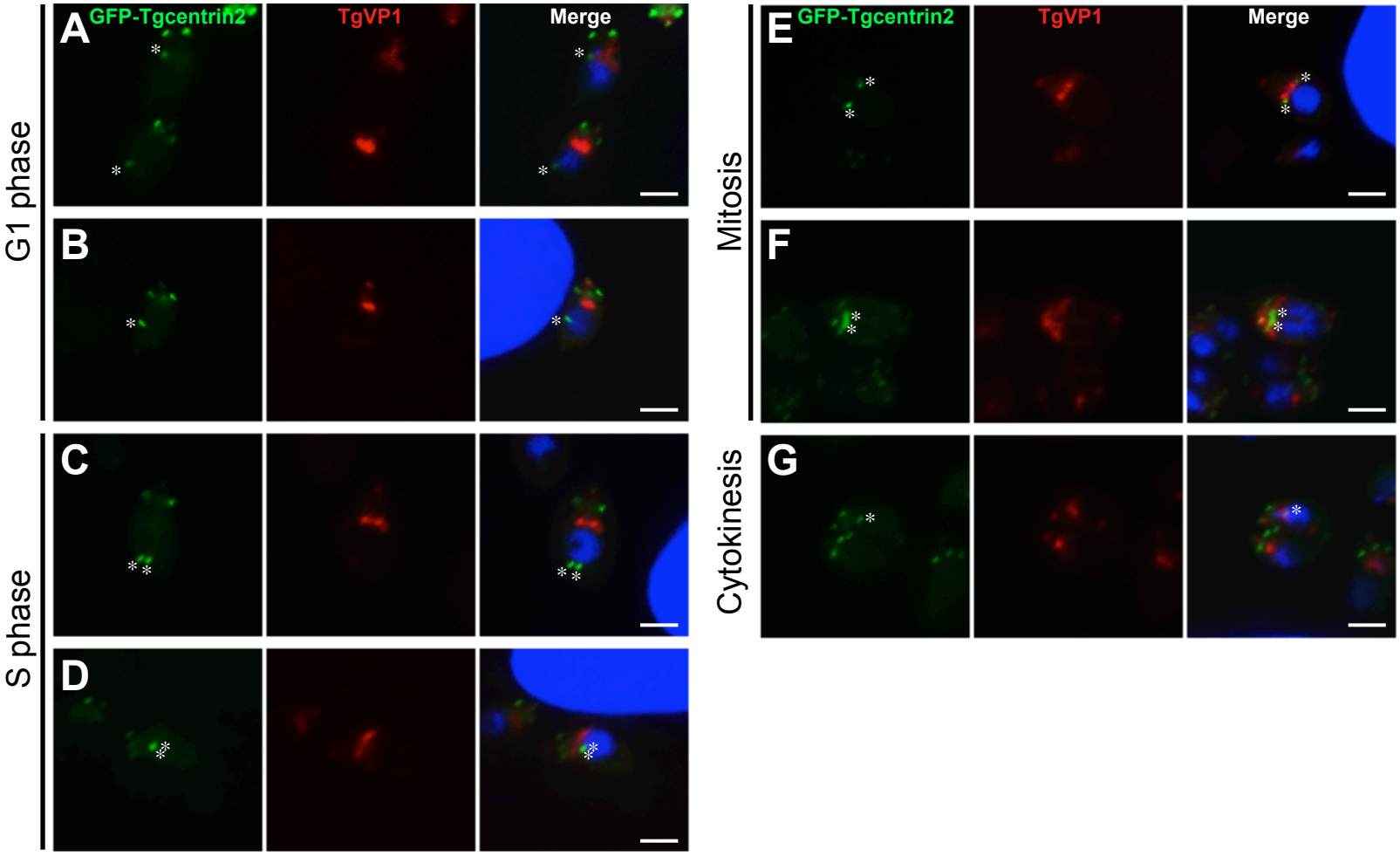
G1 phase
S phase
Mitosis
Cytokinesis
A
B
C
D
E
F
G
GFP-Tgcentrin2
TgVP1
Merge

Fig. S6

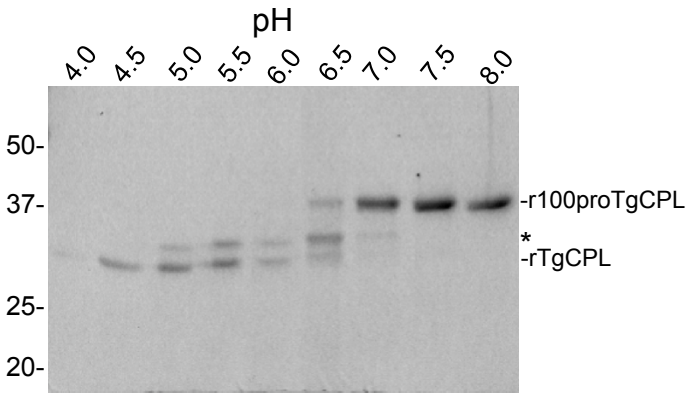

Fig. S7

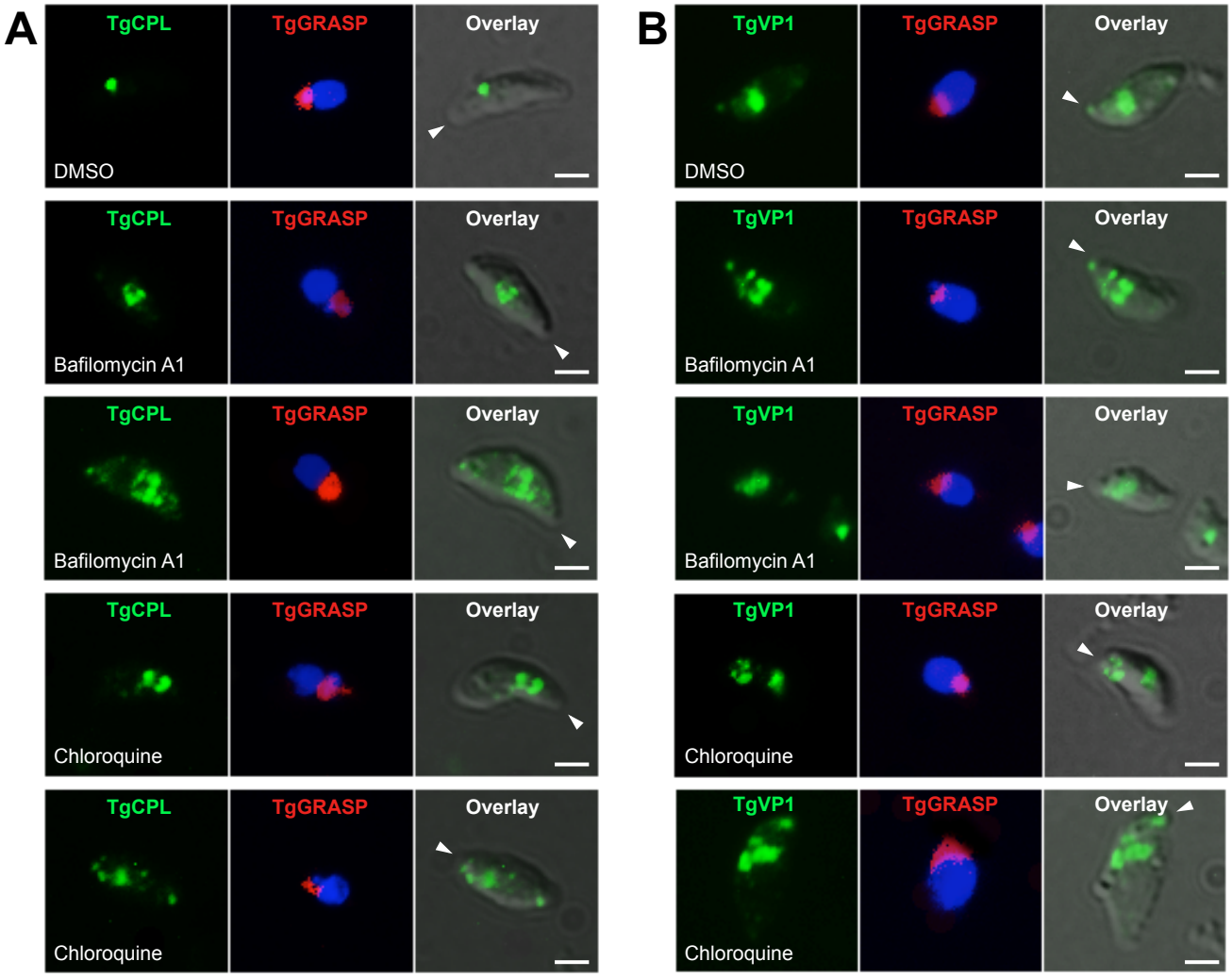
A
TgCPL
TgGRASP
Overlay
DMSO
Bafilomycin A1
Bafilomycin A1
Chloroquine
Chloroquine
B
TgVP1
TgGRASP
Overlay
DMSO
Bafilomycin A1
Bafilomycin A1
Chloroquine
Chloroquine

Fig. S8

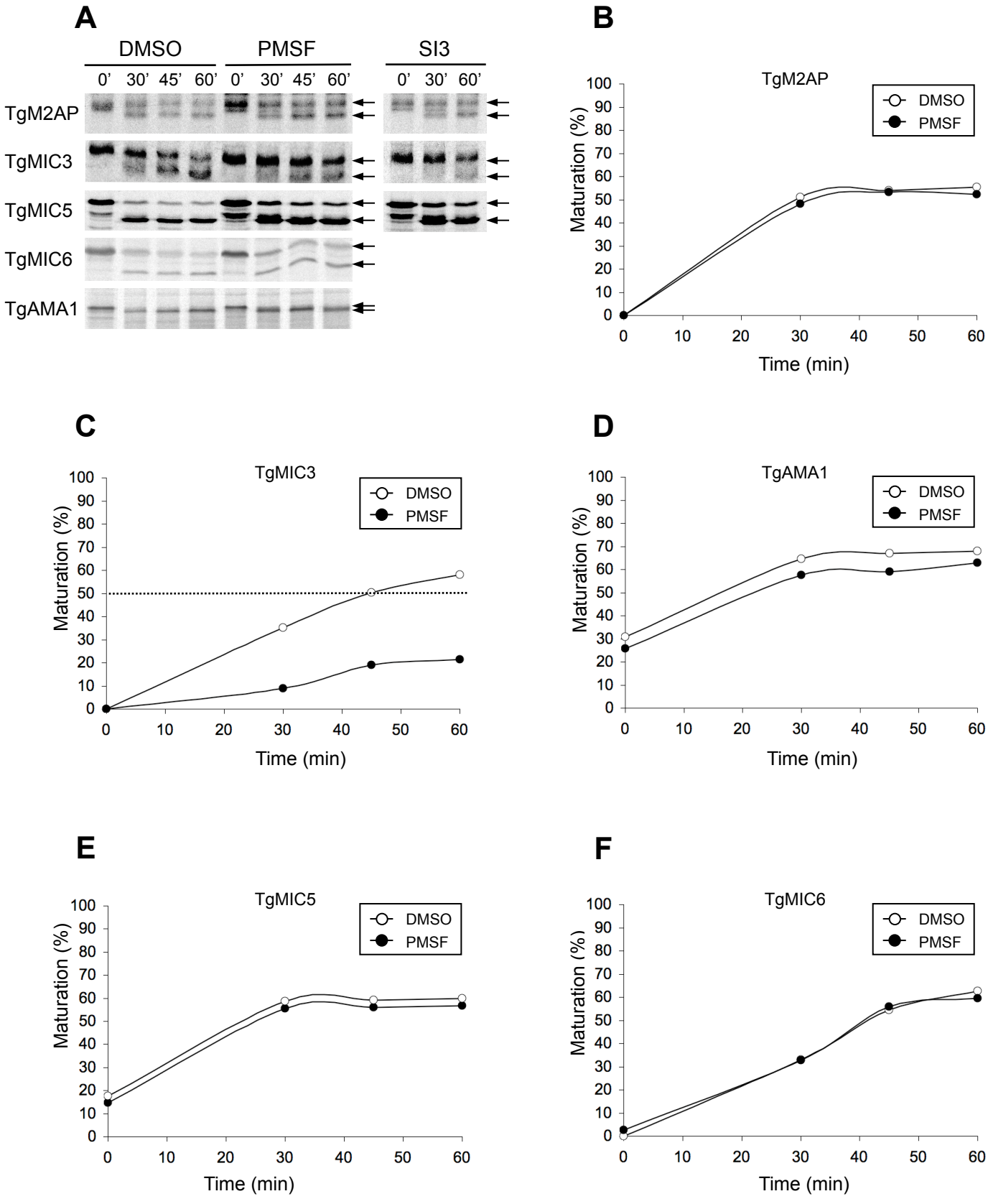
A
DMSO
PMSF
SI3
0’ 30’ 45’ 60’ 0’ 30’ 45’ 60’ 0’ 30’ 60’
TgM2AP
TgMIC3
TgMIC5
TgMIC6
TgAMA1
B
TgM2AP
DMSO
PMSF
Maturation (%)
Time (min)
C
TgMIC3
D
TgAMA1
E
TgMIC5
F
TgMIC6